Food Chemistry 259 (2018) 147–156

Contents lists available at ScienceDirect

Food Chemistry

journal homepage: www.elsevier.com/locate/foodchem

Detailed characterization of glycosylated sensory-active volatile phenols in smoke-exposed grapes and wine

Matthew Noestheden[a,b,1], Eric G. Dennis[a,1], Eduardo Romero-Montalvo[a], Gino A. DiLabio[a,c], Wesley F. Zandberg[a,*]

[a] Department of Chemistry, University of British Columbia, 3427 University Avenue, Kelowna, British Columbia V1V 1V7, Canada
[b] Supra Research & Development, 4532 Sallows Road, Kelowna, British Columbia V1W 4C2, Canada
[c] Faculty of Management, University of British Columbia, 1137 Alumni Avenue, Kelowna, British Columbia V1V 1V7, Canada

ARTICLE INFO

Keywords:
Smoke-taint
Glycosides
Wine
Grapes
Volatile phenols
Fragmentation
Accurate mass

ABSTRACT

The exposure of *Vitis vinifera* L. vines to smoke from wildland fires can alter the chemical composition of the berries, such that the resulting wine can possess a defect known as smoke-taint. This work constitutes a complete method for the analysis of simple volatile phenol glycosides (VP-glycosides) that can be elevated in berries and wine following smoke exposure. We synthesized 16 model VP-glycosides, four of which are not reported previously, to facilitate method development. Fragmentation analysis using high-resolution accurate-mass spectrometry demonstrated that the glycone and aglycone influenced the fragmentation pattern of VP-glycosides. Diagnostic fragmentation patterns for the synthesized VP-glycosides were applied to identify several VP-glycosides in smoke-exposed berries and wine. The fragmentation pattern of VP-disaccharides should facilitate the characterization of modified glycones. Putative non-VP glycosides elevated in smoke-exposed berries are demonstrated for the first time. In tandem with VP-glycosides, such compounds may contribute to the expression of smoke taint.

1. Introduction

The exposure of *Vitis vinifera* L. (*V. vinifera*) berries to smoke from wildland fires or prescribed burns can alter the chemical composition of the berries, such that the resulting wine can possess a defect known as smoke-taint. Smoke-taint is characterized by a suite of negative sensory attributes (*e.g.*, 'smoky', ashy', 'burnt meat' and 'Band-Aid' aromas and flavors) (Kennison, Gibberd, Pollnitz, & Wilkinson, 2008; Kennison, Wilkinson, Williams, Smith, & Gibberd, 2007; Ristic et al., 2016; Ristic, Pinchbeck, Fudge, Hayasaka, & Wilkinson, 2013) that have been correlated to the concentration of organoleptic volatile phenols (VPs) present within tainted wines. *In planta* and in wine, VPs are present in their free, sensory-active forms, but more dominantly they have been reported as an array of non-volatile glycoconjugates (Hayasaka et al., 2013) that, like other bound sensory-active metabolites (*e.g.,* terpenoids), possess no inherent organoleptic properties. During fermentation these VP-glycosides can be hydrolyzed to liberate the free, sensory-active VP aglycones (Kennison et al., 2008). As well, glycosidically-bound VPs can contribute to the negative organoleptic attributes of smoke-tainted wine, through in-mouth hydrolysis (Parker et al., 2012). It follows then, that an understanding of the VP-glycoside (*i.e.*, the 'sensory potential') composition of grapes is requisite when trying to predict the potential risk for smoke-exposed berries to produce smoke-tainted wine.

VP-glycosides were first reported by Hayasaka et al., who demonstrated the presence of glucosides and disaccharides in smoke-exposed berries and wine made from those berries (Hayasaka, Baldock, Pardon, Jeffery, & Herderich, 2010; Hayasaka, Baldock, Parker, et al., 2010; Hayasaka, Dungey, Baldock, Kennison, & Wilkinson, 2010), with seven putative guaiacyl glycosides proposed (Hayasaka, Baldock, Pardon, et al., 2010). While several analytical standards were synthesized to enable Level 1 annotations (Schymanski et al., 2014), most VP-glycosides were proposed based on mass differences between putative VP-glycoside precursors and common (glycone) product ions, as well as a review of glycosides postulated for other sensory-active compounds (Sarry & Günata, 2004; Wirth, Guo, Baumes, & Günata, 2001). To our knowledge, there are no published efforts to use full-scan product ion mass spectra to thoroughly characterize the VP-glycosides present in smoke-exposed berries, which is likely due, in part, to the complexity of such characterizations (Hofmann, Hahm, Seeberger, & Pagel, 2015) and

* Corresponding author at: Department of Chemistry, University of British Columbia, 3427 University Ave, Kelowna, British Columbia V1V 1V7, Canada.
E-mail address: wesley.zandberg@ubc.ca (W.F. Zandberg).
[1] MN and EGD contributed equally to this work.

https://doi.org/10.1016/j.foodchem.2018.03.097
Received 7 December 2017; Received in revised form 14 March 2018; Accepted 22 March 2018
Available online 22 March 2018
0308-8146/

a dearth of analytical standards. Nor have any definitive structures been conclusively identified for the proposed VP-glycoside isobars (Hayasaka, Baldock, Pardon, et al., 2010; Hayasaka et al., 2013) that were shown in published chromatograms. Quantitative methods using triple quadrupole mass spectrometry have been developed for the intact VP-glycosides (Dungey, Hayasaka, & Wilkinson, 2011; Hayasaka et al., 2013). However, these approaches are inherently unsuited to identify the isobaric VP-glycosides that have been proposed, as they use mass transitions that are specific to a set precursor *m/z* (*e.g.,* guaiacyl-hexose), rather than focusing on product ions that would differentiate, for instance, α- and β-anomers (Hayasaka, Baldock, Pardon, et al., 2010; Hayasaka et al., 2013). This lack of characterization is notable given the apparent importance of VP-glycosides to the expression of smoke-taint in wine. Moreover, yeast, bacterial or *V. vinifera* glycosidases are primarily responsible for the release of glycosidically-bound VPs during fermentation (Ristic, van der Hulst, Capone, & Wilkinson, 2017). As such, a detailed understanding of the glycoside chemistry could be used to inform the development of yeast with favorable enzymatic activity to mitigate the release of VP-glycosides during fermentation. It should be noted, however, that the activity of glycosidases is sensitive to small structural changes (*e.g.*, acetylation, methylation, *etc*.) in saccharide moieties (Marana, 2006); such changes are well-documented for other *V. vinifera* secondary metabolites, including terpenoids (Hjelmeland, Zweigenbaum, & Ebeler, 2015) and flavonoids. Likewise, the specific sequence of monosaccharides (*e.g.,* glucose-rhamnose-VP *vs.* rhamnose-glucose-VP) can also impact glycosidase activity, as the majority described to date are *exo*-glycosidases (Kobata, 2013).

In the present study, we synthesized a panel of representative VP-glycosides (Fig. 1) to: 1) optimize extraction and chromatographic procedures for VP-glycosides in berries and wine; 2) elucidate their collision-induced dissociation pathways using high-resolution accurate mass tandem mass spectrometry; and 3) support our hypothesis that the use of full scan, high-resolution accurate mass product ion spectra will facilitate the annotation of the, as yet, putatively identified VP-glycosides present in smoke-exposed berries and their associated wines. The new techniques described herein enabled the detection of nine VP-glycosides that were elevated in smoke-exposed berries when compared to their matched controls, providing definitive evidence for the existence of two VP-glycosides previously proposed (Hayasaka et al., 2013). The present study also demonstrates the existence of several previously unidentified VP-glycosides and supports previous research (Noestheden, Dennis, & Zandberg, 2018; Noestheden, Thiessen, Dennis, Tiet, & Zandberg, 2017) indicating that simple VP-glycosides (*i.e.*, those containing only VPs and unmodified glycones) are likely not the sole VP storage form relevant to the expression of smoke taint in wine.

2. Materials and methods

2.1. Chemicals and general details

The following chemicals were purchased from Sigma-Aldrich (Saint Louis, MO, USA) and used as received: HPLC-grade methanol (MeOH), isopropanol (IPA), acetonitrile (ACN), hexane, ethyl acetate (EtOAc), dichloromethane (CH_2Cl_2, reagent grade), and diethyl ether (Et_2O, reagent grade), 50% sodium hydroxide, anhydrous sodium carbonate, trifluoroacetic acid (TFA), acetic acid (AcOH), 2-methoxyphenol (guaiacol), 2,6-dimethoxyphenol (syringol), 2-methoxy-4-methylphenol (4-methylguaiacol), 2-methoxy-4-ethylphenol (4-ethylguaiacol), 4-ethylphenol, 2-methoxy-4-allylguaiacol (eugenol), 4-methoxyphenol, 4-methylphenol (*p*-cresol), 2-methylphenol (*o*-cresol), d_3-guaiacol, d_4-4-ethylphenol, d_5-4-ethylguaiacol, $CDCl_3$ and d_4-MeOH. Type 1 water was provided by a Barnstead E-Pure water purification system (Thermo Fisher Scientific; Waltham, MA, USA). Weighing was performed using an Adventure Pro AV264 analytical balance (Ohaus Corporation, Pinebrook, NJ, USA). A Mettler Toledo FE20 FiveEasy pH meter was used to measure pH. An Allegra X-12R centrifuge was used for sample preparation (Beckman Coulter, Mississauga, ON, Canada). Grape or wine extracts were concentrated *in vacuo* using a Savant SPD121P SpeedVac concentrator connected to a Savant RVT5105 refrigerated vapor trap (Thermo Fisher Scientific) and/or lyophilized using a Labconco Freezone 4.5 freeze dry system (Kansas City, MO, USA). Supelclean™ ENVI-Carb porous graphitic carbon (PGC) solid-phase extraction (SPE) cartridges (3 mL/250 mg) were purchased from Sigma-Aldrich. Strata-C18 E (1 mL/50 mg) and Strata-X SPE (1 mL/30 mg) cartridges were purchased from Phenomenex (Torrance, CA, USA). *Aspergillus niger* β-glucosidase (EC 3.2.1.21; 40 U/mL), α-L-rhamnosidase (EC 3.2.1.40; 1500 U/mL), β-D-xylosidase (EC 3.2.1.37; 500 U/mL) and α-L-arabinofuranosidase (EC 3.2.1.55; 300 U/mL) were purchased from Megazyme (Bray, County Wicklow, Ireland) and used as received.

Details regarding the synthesis of guaiacyl-β-D-gentiobioside, guaiacyl-α-D-glucoside, guaiacyl-β-D-xyloside, guaiacyl-β-D-primeveroside, guaiacyl-β-D-rutinoside, 4-methylguaiacyl-β-D-glucopyranoside, guaiacyl-α-L-rhamnoside, phenyl-β-D-glucopyranoside, guaiacyl-β-D-galactoside, guaiacyl-α-D-mannoside and 4-methoxyphenyl-β-D-glucopyranoside are described in the Supporting Information. The syntheses of guaiacyl-β-D-glucopyranoside, eugenyl-β-D-glucopyranoside, 4-ethylphenyl-β-D-glucopyranoside, syringyl-β-D-glucopyranoside, *p*-cresyl-β-D-glucopyranoside, and d_3-guaiacyl-β-D-glucopyranoside are reported elsewhere (Noestheden et al., 2018, 2017).

Concentrated VP, VP-glycoside and d_3-guaiacyl-β-D-glucopyranoside isotopic internal standard (ISTD) stock solutions were prepared in IPA or 1:1 IPA:H_2O at 1.0 10.0 mg/mL and stored at −20 °C. Standards were prepared fresh daily from these stocks.

2.2. Plant material

Method development was performed using Merlot berries acquired from vineyards in the Okanagan Valley (British Columbia, Canada; harvested at commercial maturity in 2016) and a commercially purchased Cabernet Franc wine produced in the Okanagan Valley in 2016. Application of the developed methods was performed on control and smoke-exposed berries (and the wine produced from these berries) from two vineyards, which were harvested in 2017. Berry samples for analysis were homogenized (HMG) in a commercial blender immediately after harvest and stored at −20 °C. Berries for wine making were stemmed and stored at −20 °C until the start of fermentation. Field trial and vinification details are described in the Supporting Information.

2.3. Sample preparation

Berry and wine extracts targeting free and acid-labile VPs were prepared using published procedures (Noestheden et al., 2018, 2017). Wine samples were dried *in vacuo* and resuspended in an equivalent volume of H_2O prior to extraction.

All samples were fortified with d_3-guaiacyl-β-D-glucopyranoside ISTD at 300 ng/mL prior to extraction. Strata-C18 E SPE cartridges were conditioned with 2 × 1 mL ACN and 2 × 1 mL H_2O, after which 1 mL of sample was loaded, washed with 1 mL H_2O and subsequently eluted with 1 mL of 40% ACN. C18 eluents that were loaded onto PGC were diluted fourfold with H_2O. ENVI-Carb SPE cartridges were conditioned with 2 × 3 mL 80% ACN, 0.1% TFA, 2 × 3 mL 0.1% TFA. After loading 1 mL of sample (or 4 mL of diluted C18 eluent) the cartridges were washed with 1 mL of 20% ACN and eluted with 1 mL of 80% ACN, 0.1% TFA. Strata-X SPE cartridges were conditioned with 2 × 1 mL ACN and 2 × 1 mL H_2O, after which 1 mL of sample was loaded and washed with 1 mL 0.1 N NaOH followed by 2 × 1 mL of H_2O. Samples were eluted with 1 mL of 40% ACN. After SPE, samples were dried *in vacuo*, resuspended in 1 mL H_2O, centrifuged for 5 min at 10,000*g* and transferred to borosilicate glass vials for analysis.

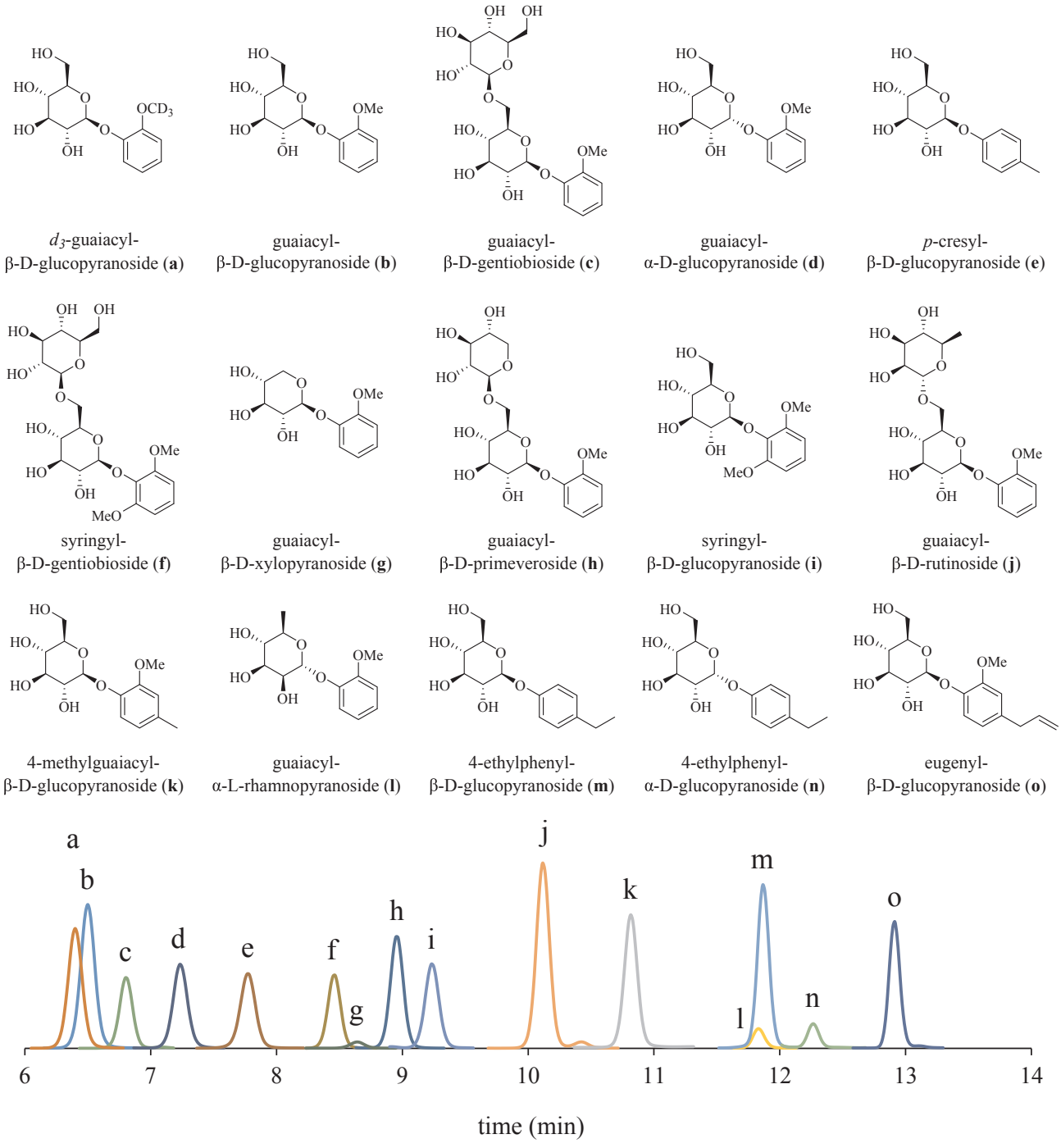

Fig. 1. Structures of model VP-glycosides synthesized (top). Sample chromatogram obtained from a standard mixture containing 200 ng/mL of each model VP-glycoside (bottom).

2.4. Exo-glycosidase digests

Following SPE using the Strata-X procedure (Section 2.4), a berry extract from the smoke-exposed sample group was aliquoted (100 µL) into 1.5-mL polypropylene centrifuge tubes, to which 10 µL of BSA (1 mg/mL) and 5 µL of buffer (1 M; see below) were added. A mixture of model glycosides (Table S1) was fortified (2 µL) into buffer and berry extract at 200 ng/mL in duplicate, with one set of samples receiving enzyme (positive control) and the other receiving no enzyme (negative control). One set of extracts was also prepared with and without enzyme. Therefore, each enzyme digest consisted of six reactions: positive and negative controls fortified with model glycosides in buffer and in extract, as well unfortified extract with and without enzyme. Final enzyme reaction conditions were: 25 µL β-glucosidase, 50 mM NaOAc, pH 4, 70 °C; 1 µL α-L-rhamnosidase, 50 mM $NaPO_4$, pH 6, 45 °C; 1 µL β-D-xylosidase, 50 mM NaOAc, pH 4, 45 °C; and 3 µL α-L-arabinofuranosidase, 50 mM NaOAc, pH 4, 45 °C. Digests were performed for 24 h, after which 850 µL of water were added to each reaction and the resulting mixtures were purified (Strata-C18 E procedure in Section 2.4). After drying *in vacuo*, samples were resuspended in 100 µL water and centrifuged for five min at 12,000*g*. The resulting supernatant was analyzed by uHPLC-QToF (Section 2.7) without further work-up.

2.5. Computational details

Density functional theory (DFT) modeling was performed for selected VP-glycosides (Fig. 1[b, e, i, k, m and o]) and their corresponding fragmentation products. The $[M-H]^-$ ion of each VP-glycoside served as the initial structure for optimization calculations. The most acidic gas phase proton was determined. Fragmentation was assumed to occur *via* concerted elimination on C1/C2 of the glycone (see Section 3.4.2). The level of theory used was M06-2X/6-31 + G(d,p) (Hehre, Ditchfield, & Pople, 1972; Zhao & Truhlar, 2008) by means of the Gaussian-09 Rev.D.01 program (Frisch et al., 2009). Subsequent harmonic frequency computations confirmed that all geometries are genuine minima on their respective potential energy surfaces (PES).

2.6. GC–MS/MS

Analyses were performed on a TSQ™ 8000 Evo Triple Quadrupole GC–MS/MS equipped with a TRACE 1310 GC and TriPlus RSH autosampler (Thermo Fisher Scientific). The carrier gas was helium (99.999%). The injection port temperature was 220 °C. A 5-µL injection volume was used for all analyses. Quantitative analyses were performed on an SLB-5 60 m × 0.25 mm × 0.25 µm capillary column (Sigma Aldrich) using a splitless single-taper liner (4.0 mm I.D., 6.2 × 78.5 mm; Restek, Bellefonte, PA, USA). The transfer line and source temperatures were 280 °C and 300 °C, respectively. The GC temperature program and MS/MS parameters used were exactly as described by Noestheden et al. (2018)).

2.7. uHPLC-QToF

uHPLC was performed using an Agilent 1290 Infinity system (Agilent Technologies; Santa Clara, CA, USA) equipped with a 1290 Infinity binary pump, 1290 Infinity autosampler and a 1290 Infinity thermostated column compartment. A needle wash solution of 2:1:1 IPA:MeOH:H_2O was used, with a 3-s wash during each injection cycle. Samples were analyzed using a 20-µL injection on a Luna Omega C18 50 × 2.1 mm, 1.6 µm column (40 °C). Gradient and mobile phase conditions are summarized in Table S2.

Mass spectrometry was performed on an Agilent 6530 QToF equipped with a Jet Stream electrospray ionization (ESI) source operated in negative ion mode. Full scan data (10,000 resolution at *m/z* 118.0863; 20,000 resolution at *m/z* 622.0287) were acquired from *m/z* 65–1000 at a scan rate of 1 Hz. CID experiments were performed at 5, 10, 20 and 40 V collision energy (CE) using targeted MS/MS acquisition, with data collected from *m/z* 50–1000 at a scan rate of 2 Hz. MS parameters are summarized in Table S3 and a summary of the model glycoside formulae, retention times and ions evaluated are provided in Table S1.

2.8. Method performance

The method detection limits (MDL) for model glycosides were estimated based on a peak-to-peak signal-to-noise ratio ≥3 for berry and wine samples fortified at 20 or 50 ng/mL prior to extraction.

2.9. Data acquisition and processing

GC–MS/MS data were processed using the Xcalibur (v 3.0.63) and TraceFinder (v 3.2.512.0) software packages (Thermo Scientific). The uHPLC-QToF data acquisition and processing were carried out using the MassHunter Workstation software suite (Agilent Technologies), with version numbers as follows: Data Acquisition Workstation (v B.06.01, Service Pack 1), Qualitative Analysis (v B.07.00, Service Pack 2). A combinatorial database containing 1430 compounds with 407 unique neutral monoisotopic masses for reported and plausible VP-glycosides (Table S4) was created to process samples. The MassHunter find-by-formula algorithm was used to search for VP-glycoside precursor ions ($[M+AcO]^-$). Extracted ion chromatograms were generated with a ± 10 ppm mass window and Gaussian smoothing was applied prior to integration with the Agile2 integration algorithm.

3. Results

3.1. VP-glycoside chromatography

Contrary to published methods that utilized ACN as an organic eluent (Hayasaka, Baldock, Pardon, et al., 2010; Hayasaka, Baldock, Parker, et al., 2010; Hayasaka, Dungey, et al., 2010), herein we used MeOH, reasoning that a solvent with a lower eluotropic strength would facilitate retention of the polar VP-glycosides on a C18 stationary phase. Coupled with an isocratic hold at 2% organic followed by a two-step gradient to 15% organic at 10 min, this approach yielded a retention factor of 30 for the first eluting VP-glycoside at 6.4 min (Fig. 1, **a**), with all model VP-glycosides eluting in 13 min. While it would be possible to increase the throughput of this method for routine testing, the current application was to screen for and characterize VP-glycosides. The demonstrated presence of multiple isobars (Hayasaka, Baldock, Pardon, et al., 2010; Hayasaka, Baldock, Parker, et al., 2010) for several VP-glycosides warranted a conservative chromatographic separation to facilitate characterization.

3.2. Solid-phase extraction of model VP-glycosides from berries and wine

The use of C18 SPE sorbents has been reported for the extraction of VP-glycosides from whole berry homogenate (Hayasaka, Baldock, Pardon, et al., 2010), while VP-glycosides in wine have been analyzed directly after simple filtration (Hayasaka, Baldock, Parker, et al., 2010). In the current study, these approaches resulted in recoveries of 0–43%, with mean recoveries of 15% and 24% from C18 and filtration-based approaches, respectively (Fig. 2, Table S5). These low recoveries are primarily attributed to ion suppression, since solvent extracts performed using the same procedures demonstrated quantitative recovery and matrix extracts fortified after SPE showed similar responses to samples fortified before SPE (data not shown). Based on these preliminary results, it was deemed necessary to evaluate SPE sorbents with orthogonal separation and chemical stabilities to facilitate adequate sensitivity for characterizing VP-glycosides in smoke-exposed berries and wine using uHPLC-QToF mass spectrometry. This included the use of porous graphitic carbon (PGC), two orthogonal SPE sorbents (C18 and PGC) in series and an alkaline-stable polymeric sorbent (Strata-X; Fig. 2, Table S5).

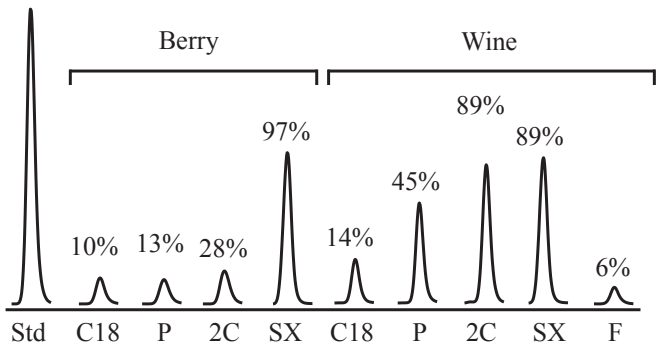

Fig. 2. Solid-phase extraction of whole berry homogenate and wine after fortification with model VP-glycosides at 200 ng/mL. Sample chromatograms (same *y*-axes) are shown for d_3-guaiacyl-β-D-glucopyranoside. A tabular summary of absolute recoveries for all model VP-glycosides is provided in Table S5. Std – unextracted control; C18 – Strata-C18-E (50 mg/1 mL); P – ENVI-Carb (250 mg/3 mL); 2C – C18 eluent loaded onto to ENVI-Carb; SX – Strata-X (30 mg/1 mL) polymeric phase; F – 0.2 µm filter prior to analysis.

The utility of PGC was evaluated based on the retention of polar analytes being stronger than a standard C18 sorbent, which would permit washing of the sorbent after sample loading with a stronger eluotropic solvent to remove matrix components. For example, the C18 sorbent was only compatible with an H_2O wash following sample loading without loss of VP-glycosides. On the other hand, it was determined that PGC could be washed with 20% ACN without the loss of VP-glycosides. With recoveries of 17–53% and a mean recovery of 35%, PGC performed better than the C18 sorbent (Fig. 2, Table S5). However, the recoveries were still low.

To leverage the different retention mechanisms of C18 and PGC, the two sorbents were used in series. This two-column solution was promising (mean recovery = 70%), but the spread of recoveries was 16–147%, demonstrating unacceptable variability in the behavior of the different VP-glycosides (Fig. 2, Table S5). One potential reason for this was postulated to be the co-elution of monomeric flavonoids and their glycosylated analogs causing ion suppression, despite sample clean-up on two sequential columns, since they bear chemical similarity to VP-glycosides (and thus may elute from SPE and HPLC columns under similar conditions) and are present in berries and wine at high concentrations. In the present study, the Strata-X cartridge was washed with 0.1 N NaOH (pH 13) to deprotonate and broadly remove polyphenolic flavonoids and their glycosides from the SPE sorbent after sample loading. The VP-glycosides would be expected to be retained on the SPE sorbent, since they lack suitably acidic protons to behave as polyphenolics (*i.e.*, the phenolic proton is not present due to the formation of a glycosidic bond). A similar approach was recently utilized to remove polyphenolic compounds as part of a sensory study in wine (Parker et al., 2017). Given the reported stability of VP-glycosides in 0.2 M NaOH (pH 11.5) for 4 h at 100 °C (Noestheden et al., 2018), the alkaline SPE wash was not expected to adversely impact method recoveries for VP-glycosides. This approach yielded the most promising data, with recoveries of 58–127% and a mean recovery of 89% (Fig. 2, Table S5). Comparing matrix extracts fortified before and after SPE using the Strata-X sorbent and an alkaline wash demonstrated ion suppression of 0–52%. On aggregate, this procedure yielded the best results, so it was carried forward for the approximation of MDLs (Section 3.3) and the analysis of smoke-exposed berries and the wine made from those berries (Section 3.5).

3.3. Approximating method detection limits

Using the optimized SPE procedure on the Strata-X sorbent with alkaline sample wash, the model VP-glycosides were fortified into whole berry homogenate and wine at 20 and 50 ng/mL to estimate the method detection limits (MDLs). Using a peak-to-peak signal-to-noise ≥ 3, the MDLs for model VP-glycosides were 2–20 ng/mL (Fig. 3), except for guaiacyl-β-D-primeveroside in berries and wine and guaiacyl-α-L-rhamnoside in wine, which were 50 ng/mL. The limit-of-quantitation reported for d_3-syringyl-gentiobioside in berries (1.8 ng/mL after dilution factor adjustment (Hayasaka et al., 2013)) was similar to the MDL reported herein (2 ng/mL) for syringyl-gentiobioside (Fig. 3). While this showed that the current method was not as sensitive, the respective MDLs herein were still applicable for the analysis of VP-glycosides, given their reported concentrations in smoke-exposed berries of 0.02–7 μg/mL (Hayasaka, Baldock, Parker, et al., 2010; Hayasaka et al., 2013).

3.4. MS/MS fragmentation analysis of model VP-glycosides

3.4.1. General VP-glycoside fragmentation

MS/MS analysis of putatively identified VP-glycosides and those confirmed from analytical standards were concerned with the assignment of transitions suitable for quantitative multiple-reaction monitoring methods (Dungey et al., 2011; Hayasaka et al., 2013). While appropriate for the intended application, this approach neglected the less abundant features of the product ion spectrum, which are invaluable for the proposal of plausible structures for unknown compounds in the absence of analytical standards, and as potential markers to improve specificity during screening studies. Such analyses are especially relevant to VP-glycosides, as there can be several isobars for a given glycone-aglycone pair (*e.g.*, β1–6, β1–4, *etc*. for disaccharide linkages), in addition to the possibility of modified glycones (*e.g.*, acylations) that could impact VP-glycoside metabolism (and subsequent release of the organoleptic free VPs) during fermentation and aging.

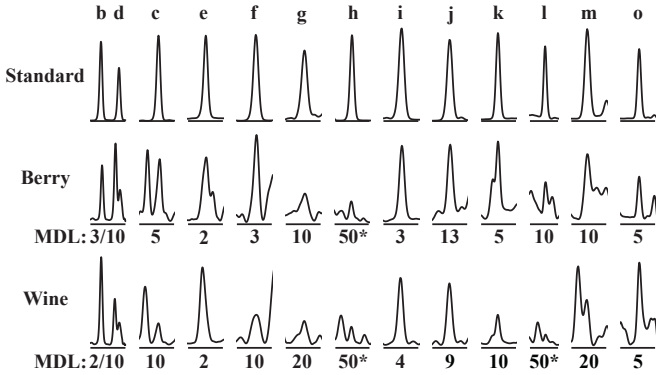

Fig. 3. Method detection limits (MDLs, ng/mL) for model VP-glycosides were based on fortified berry and wine extracts that were extrapolated to a signal-to-noise ≥ 3 (peak-to-peak). Compound designations reference Fig. 1. * Indicates 50 ng/mL fortification; all other MDLs were determined after 20 ng/mL fortifications. Chromatograms do not share *y*-axes.

The series of VP-glycosides analyzed herein (Fig. 1) was designed to cover a range of glycone-VP permutations including: 1) α- *versus* β-anomers; 2) a constant glycone with variable VP for mono and disaccharides; and 3) a constant VP with variable glycone for mono and disaccharides. Using the fragmentation nomenclature established by Domon and Costello (1988), detailed analyses of model VP-glycosides were conducted (Figs. 4 and S1–S4). A range of applied collision energies was used to generate information-rich full scan product ion spectra, with the goal of building sets of key fragments that would assist in the verification of putatively identified VP-glycosides. It was also postulated that these key fragments could be used as screening tools for unreported VP-glycosides, including the presence of modified glycones, as has been reported for flavonoids and terpenoids (Fanzone et al., 2012; Hjelmeland, Zweigenbaum, & Ebeler, 2015).

Some data has been reported for VP-glycosides in tomato using accurate mass, but full product ion spectra were not published in this work (Tikunov et al., 2013). The only full product ion spectrum (nominal mass resolution) reported to date for VP-glycosides was for guaiacyl-β-D-glucopyranoside (Hayasaka, Dungey, et al., 2010). In this case, the primary fragmentation pathway appeared to be neutral loss of the acetate adduct (likewise, all VP-glycosides studied herein ionized as acetate adducts in negative ESI) to yield the deprotonated molecular ion, which then favored the formation of a B_1 fragment with corresponding neutral loss of the aglycone. Hayasaka et al. also provide evidence for the neutral loss of the glycone to yield a corresponding Y_0 (guaiacylate) ion and potentially a couple of ions relating to the fragmentation of glucose, although these are difficult to confirm in the absence of the raw data. Broadly, the data herein agreed with that of Hayasaka, et al., with B_1 ions dominating at lower collision energies and a conversion to Y_0 ions as the applied potential increased (Fig. S1). However, there were additional product ions that provided information about the glycone, with $^{2,5}A_1$, $^{1,3}A_1$, $^{0,4}A_1$, $^{1,5}A_1$ and $^{3,5}A_1$ ions indicative of the fragmentation of glucose. Indeed, at a collision energy of 20 V, the product ion profile favored these higher-order fragments over B_1 ions (Fig. 4, **b**). Such ions are integral to characterizing unreported VP-glycosides, especially those that might contain modified glycones, as the presence/ratio of these ions would be expected to change due to

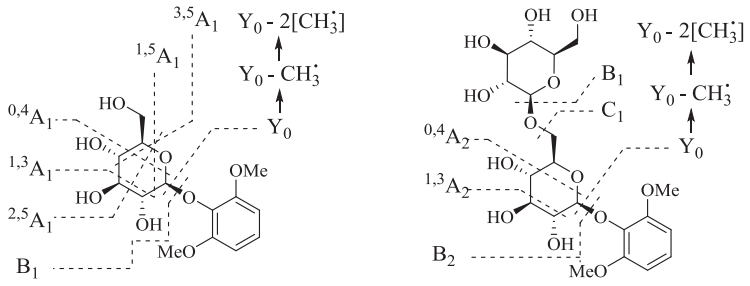

Fig. 4. Representative CID fragmentation for glycosidically-bound volatile phenol mono- (top left) and disaccharides (top right). For clarity, fragmentation of the non-reducing sugar of the disaccharide and of the $[M+AcO]^-$ precursors to $[M-H]^-$ ions are omitted. Product ion responses (bottom, CE = 20 V) are reported as a fraction of the total ion current for all proposed fragments ($^{0,4}A_1$ excluded due to multiple plausible sources, including decomposition of $[M+AcO]^-$ precursor ions). Mass accuracy and absolute abundance details can be found in Tables S7 and S8. Complete fragmentation analyses and spectra are in Figs. S1–S14.

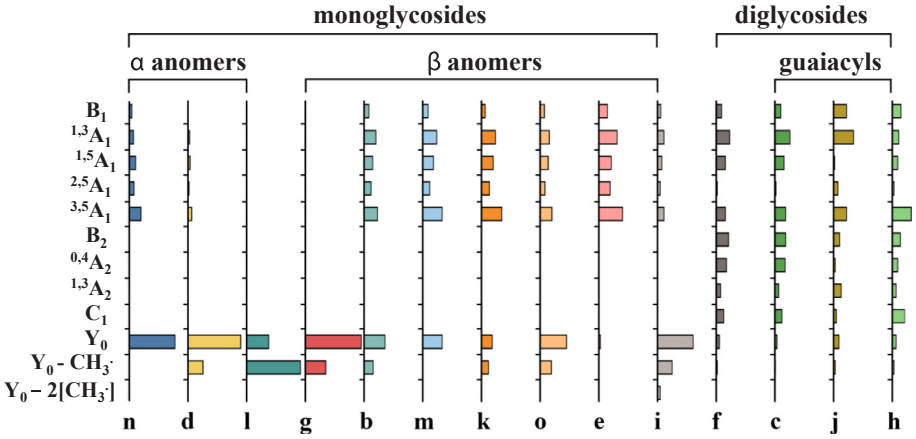

the glycone modification. Similar B_1/Y_0 and glucoside product ions were observed for the other β-D-glucosides analyzed (Figs. 4 **[m, k, o, e, i]**, S4, S8, S10, S12 and S14).

Another interesting feature of the product ion spectra for **b** was the apparent homolytic cleavage of the *ortho*-methoxy group of the Y_0 ion to yield a radical anion ($Y_0 - CH_3^{\cdot}$; Figs. 4 and S1). At high collision energies, this fragment dominated the product ion spectrum. Comparison to the other guaiacyl-type (**k**, **o** and **f**, Figs. S10/S14) glycosides demonstrated that this fragmentation pathway was present when *ortho*-methoxy groups were introduced to the aglycone. Syringyl-glycosides (**f** and **i**, Figs. S5/S8) also showed this pathway, as well as a product ion corresponding to the loss of an additional methyl radical to yield a $Y_0 - 2[CH_3^{\cdot}]$ ion. With an applied collision energy of 20 V, the Y_0 and $Y_0 - CH_3^{\cdot}$ ions were the dominant fragments for **i** (Fig. 4). Similar homolytic fragmentation has been reported for methoxylated/polymethoxylated and glycosylated flavonoids (Justesen, 2001; Yang et al., 2014) and hydroquinone glycosides (Liu, He, Zhang, Shi, & Abliz, 2009). For the hydroquinone glycosides, these radical anions were used to differentiate glycosidic positional isomers and for flavonoids they were diagnostic of 3-*O*-glycosylated derivatives. In the present application, $Y_0 - CH_3^{\cdot}$ ions are diagnostic fragments for guaiacyl-type and syringyl aglycones. It should be noted that high-resolution MS analysis is required to differentiate guaiacyl and syringyl fragments (see Section 3.5), as the syringyl $Y_0 - 2[CH_3^{\cdot}]$ (*m/z* 123.0088) ion is nominally the same *m/z* as the guaicylate ion (*m/z* 123.0452).

Despite the noted diagnostic utility of these radical anions, little is currently known about their plausible gas-phase structure, with existing literature discussing them as 'stable' radicals (Justesen, 2001). To better understand the nature of the gas-phase stability of these atypical ions, DFT-based calculations were performed. The bond lengths and associated geometries determined for these VP-glycoside systems using DFT calculations are summarized in Table S6. In addition to being stable structures and true minima on the PES, these radical anions are close to symmetrical, with C—O distances of 1.25 Å in all cases. This indicated that charge delocalization occurs in these ions, as might be expected for hydroquinone-type structures.

The thermodynamic data reported in Fig. S15 revealed that, for the β-anomers considered, the formation of B_1 fragments is more spontaneous than the formation of Y_0 fragments. This result agreed with the fact that at lower collision energies B1 fragments were more abundant.

3.4.2. Glycoside anomeric configuration

Comparing the fragmentation of the α-anomers for guaiacyl (**d**) and 4-ethylphenyl (**n**) glucosides showed striking differences in the observed product ions when contrasted against the MS/ MS spectra of their β-anomers (**b** and **m**, respectively; Fig. 4). For both aglycones, the α-anomers fragmented almost exclusively to Y_0 ions at all collision energies (Figs. S3/S13). Indeed, based on these data, α- and β-anomers could be assigned based on the ratio of Y/(A + B) fragments. In this semi-quantitative approach, a ratio > 1 would suggest an α-anomer. Similar results were obtained for guaiacyl-α-L-rhamnoside (**l**), which bears the same configuration at the anomeric carbon (Figs. 4 and S11). Mechanistically, Y_0 ions for α-anomers likely form *via* a concerted elimination of the aglycone by formation of an oxacarbenium species. This fragmentation pathway is facile due to the favorable secondary molecular orbital interactions possible for the α-anomers. Contrary to this pathway, β-anomers can form Y_0/B_1 product ions *via*: 1) C4/C5 epoxide formation from the $[M-H]^-$ ion, with ring opening and elimination of the aglycone followed by proton transfer (Y_0 formed prior to proton transfer to form B_1) (Domon & Costello, 1988); or 2) *via* a concerted C1/C2 elimination to directly yield B_1. It is likely that both mechanisms contribute to the reported β-anomer fragmentation. This strong difference in fragmentation pathways for α and β-anomers could be utilized to assign the anomeric chemistry of unknown VP-glycosides (see Section 3.5). Similar results were recently published using spectroscopic discrimination of carbohydrate product ions (Schindler et al., 2017) and ion-mobility mass spectrometry (Hofmann et al., 2015). But these techniques required non-standard instrumentation, whereas the results here can be obtained using a conventional MS configuration.

3.4.3. Guaiacyl glycosides

The investigation of the tandem MS spectra of α- and β-anomers of

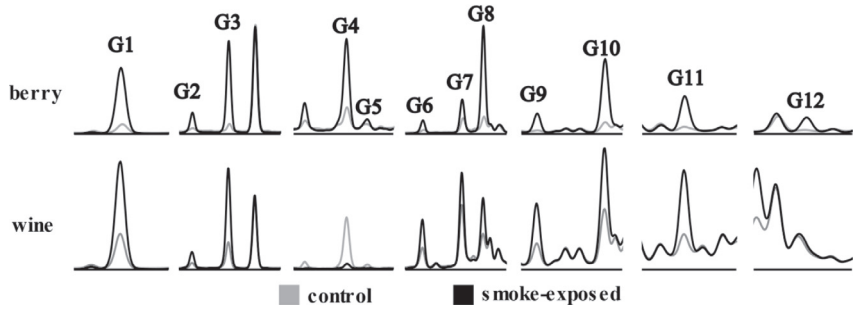

#	formula (ppm)	RT (min)	aglycone *m/z* (ppm)	glycone *m/z* (ppm)	compound ID
G1	$C_{12}H_{16}O_6$ (-1.3)	3.3	93.0352 (6.4)	161.0469 (8.7) [1]	phenyl-β-D-glucoside [2]
G2	$C_{13}H_{18}O_7$ (0.6)	5.7	123.0454 (0.8) 108.0215 (-4.6)	161.0444 (5.8) [1]	unknown glucoside
G3	$C_{13}H_{18}O_7$ (-1.2)	6.5	123.0453 (1.7) 108.0212 (-1.9)	161.0464 (-6.8) [1]	guaiacyl-β-D-glucopyranoside [2]
G4	$C_{13}H_{18}O_7$ (-3.2)	7.3	123.0449 (-2.4)	-	unknown glucoside
G5	$C_{13}H_{18}O_7$ (1.4)	7.7	123.0438 (-11)	-	unknown glucoside
G6	$C_{17}H_{24}O_{10}$ (2.5)	4.8	153.0559 (1.3)	-	unknown arabinoside
G7	$C_{17}H_{24}O_{10}$ (0.4)	5.8	93.0333 (-14)	293.0861 (5.8) [3] 161.0453 (-1.2)	phenyl-hexose-pentoside
G8	$C_{17}H_{24}O_{10}$ (1.6)	6.3	93.0351 (5.4)	293.0871 (-2.4) [3] 161.0480 (16)	phenyl-β-D-glucose-xyloside
G9	$C_{18}H_{26}O_{11}$ (0.2)	7.7	123.0447 (-4.1) 108.0221 (3.7)	293.0905 (9.2) [3]	guaiacyl-β-D-glucose-arabinoside
G10	$C_{18}H_{26}O_{11}$ (1.0)	8.7	123.0469 (14) 108.0223 (5.6)	293.0895 (5.8) [3] 161.0480 (16)	guaiacyl-β-D-glucose-xyloside
G11	$C_{19}H_{28}O_{11}$ (1.0)	10.1	123.0442 (-8.1) 108.0222 (4.6)	307.1000 (-13) [3] 163.0599 (-8.6)	guaiacyl-rutinoside [2]
G12	$C_{19}H_{28}O_{12}$ (3.9)	6.7	123.0436 (-8.1) 108.0205 (-11)	323.0974 (-3.1) [3] 161.0442 (-8.1)	guaiacyl-gentiobioside [2]

[1] plus $^{1,3}A_1$, $^{1,5}A_1$, $^{2,5}A_1$, $^{3,5}A_1$
[2] retention time match for respective model VP-glycosides
[3] plus $^{1,3}A_1$, $^{1,5}A_1$, $^{2,5}A_1$, $^{3,5}A_1$, $^{0,4}A_2$, $^{1,3}A_2$, C_1

Fig. 5. Compounds identified from a VP-glycoside database as elevated in smoke-exposed relative to control samples from vineyard 1. Chromatograms (top) are scaled to the same *y*-axis for each compound and were generated as output from the Find-by-Formula algorithm of the MassHunter software.

VP-glycosides demonstrated a difference between guaiacyl glucosides and rhamnosides, with the latter producing Y_0 ions almost exclusively due to the stereochemistry of the anomeric center (Section 3.4.2). To further investigate the impact of the glycone on fragmentation, we synthesized **g** as a representative pentosyl glycoside containing a β-anomeric configuration. Note that apiosides, xylosides and arabinosides are all known conjugates of terpenoids/flavonoids and simple phenolics in berries and wine (Barnaba et al., 2016; Hjelmeland & Ebeler, 2015). Comparisons between the guaiacyl glucoside (β anomer), rhamnoside and xyloside showed that the rhamnoside and xyloside response factors were approximately 5-fold lower than for the glucoside (Fig. 1). This result was postulated to originate from the lack of the C_6-hydroxyl group, which appeared to have a role in the generation of the acetate-adduct that subsequently fragments to the deprotonated molecular ion. Regardless of the lower response factors, the approximate MDLs (Section 3.3) for **g** and **l** demonstrated that screening for such VP-glycosides was still feasible. Also unique to **g** and **l**, were the fact that they both exclusively produced Y_0 (and $Y_0 - CH_3$) ions. For **g**, this was a function of the rhamnoside anomeric chemistry. For **l**, the low product ion responses (Fig. S8) suggested that Y_0 ions were formed through an alternate, unfavorable reaction pathway.

3.4.4. Guaiacyl and syringyl disaccharides

Disaccharides have been reported as the dominant form of VP-glycosides in smoke-exposed berries and smoke-tainted wine (Hayasaka et al., 2013). To investigate their fragmentation, we synthesized three guaiacyl disaccharides (**c**, **j** and **h**, Fig. 1) as surrogates for the putatively identified VP-disaccharides, as well as syringyl-gentiobioside (**f**, Fig. 1).

The guaiacyl and syringyl gentiobiosides (Fig. 4) showed similar fragmentation patterns, with both yielding glycone fragments of the reducing sugar ($^{1,3}A_2$, $^{0,4}A_2$) and fragmentation of the interglycosidic bond (C_1; Fig. 4). Both compounds also showed fragmentation of the non-reducing sugar that was similar to that observed for the glucosides (Section 3.4.1). These results suggested that, contrary to the results of the monoglycosides, the aglycone does not have a relevant impact on the fragmentation of disaccharides (see Section 3.5).

Comparison of the guaiacyl rutinoside and primeveroside to the gentiobioside demonstrated broadly similar product ions, regardless of the identity of the non-reducing sugar or interglycosidic bond configuration (Figs. 4 [**c**, **j**, **h**], S2, S7 and S9). While there were modest differences in the observed product ion ratios, in general the disaccharides fragmented similarly. This will present a challenge when trying to differentiate the isobars of unmodified VP-disaccharides based on the glycone fragmentation. However, since the fragmentation

profiles covered both the glycone and aglycone, the detailed product ion characterization herein could facilitate the investigation of putatively identified and unreported VP-glycosides when glycone modifications are present.

3.5. VP-Glycoside screening

3.5.1. Smoke-exposed berries

To explore the utility of the established VP-glycoside fragmentation pathways, Pinot noir berries that were exposed to experimentally produced smoke and matched, unsmoked control berries were analyzed from two vineyards in the Okanagan Valley of British Columbia, Canada. After preparing extracts via the optimized Strata-X SPE procedure, the samples were analyzed for VP-glycosides using a combinatorial database containing 1430 compounds with 407 unique neutral monoisotopic masses that covered seven unique VP monoisotopic masses (Table S4). This comprehensive database contained the common modifications reported for terpenoids, flavonoids and VPs in *V. vinifera* and the model VP-glycosides discussed herein.

Interrogation of the Pinot noir berries using this combinatorial database identified 12 putative simple VP-glycosides that were present at higher levels in smoke-exposed *versus* unsmoked controls across both vineyards (Fig. 5; based on precursor ion response). Three of these compounds matched the retention time and fragmentation patterns of model VP-glycosides discussed herein: guaiacyl-β-D-glucopyranoside (**G3**), guaiacyl-rutinoside (**G11**) and guaiacyl-gentiobioside (**G12**). The glucopyranoside of guaiacol was previously identified in smoke-exposed berries using an analytical standard (Hayasaka, Dungey, et al., 2010). The gentiobioside and rutinoside of guaiacol were putatively identified (Hayasaka, Baldock, Pardon, et al., 2010; Mayr et al., 2014), so the evidence presented herein represents the first Level 1 (Schymanski et al., 2014) annotation of these metabolites in smoke-exposed berries using reference standards and detailed high-resolution accurate mass fragmentation analysis.

Three phenyl-glycosides (**G1**, **G7**, **G8**) and two guaiacyl-hexose-pentosides (**G9**, **G10**) were also putatively identified (Fig. 5). Fragmentation analysis of **G1** supported a phenyl-β-hexoside, although it did not permit the identification of the hexose (see Section 3.4.3). Subsequent synthesis of phenyl-β-D-glucopyranoside (Figs. S19/S20) demonstrated a retention time and fragmentation match for **G1**. Moreover, **G1** was also sensitive to β-glucosidase (Fig. S16), leading to the confirmed annotation of phenyl-β-D-glucopyranoside in the smoke-exposed berries and wine evaluated herein.

G7 and **G8** fragmentation data supported their plausible identities as phenyl-hexose-pentosides, which were previously reported in smoke-exposed berries (Hayasaka, Baldock, Parker, et al., 2010). Identification of these compounds was important, since hexose-pentose glycosides were reported as the most abundant VP-glycosides in smoke-exposed *V. vinifera* (Hayasaka, Baldock, Parker, et al., 2010; Hayasaka et al., 2013). Enzymatic analysis of **G8** with β-D-xylosidase and α-L-arabinofuranosidase confirmed that it was a terminal xyloside (Fig. S16). Subsequent manual fractionation of **G8** from a total berry extract and re-analysis with β-D-xylosidase demonstrated an increase in phenyl-β-D-glucopyranoside, confirming the identity of **G8** as a phenyl-β-D-glucose-xyloside. While it is most probable that this represents a primeveroside, the exact glycosidic linkage between glucose and xylose is still under investigation. Applying a similar workflow to **G7** suggested a possible terminal apiose, since **G7** was resistant to both β-D-xlyosidase and α-L-arabinofuranosidase (Fig. S16). Additional analyses are required to definitively annotate this VP-glycoside.

G9 and **G10** fragmentation supported guaiacyl-hexose-pentosides (Fig. 5). Comparison of the glycone fragmentation data to that of **h** (Fig. 4) did not demonstrate diagnostic differences that would facilitate the assignment of plausible structures, although a difference in retention time between **h** and **G9**/**G10** confirmed that these were not primeverosides. Like **G7** and **G8**, enzymatic analyses of **G9** and **G10** with β-D-xlyosidase and α-L-arabinofuranosidase permitted their identification as a terminal arabinoside and xyloside, respectively (Fig. S16). Subsequent fractionation of these compounds and enzymatic digestion confirmed the identity of the hexose as β-D-glucose in both instances. **G10** represents the first confirmation of a disaccharide isomer containing a VP. The combinatorial database used herein contained a variety of common glycoside modifications, including esterification of the glycone by small organic acids and hydroxycinnamates. Screening of the smoke-exposed Pinot noir samples revealed putative matches for VP-glycosides with modified glycones, but in all instances they were present at similar concentrations in control and smoked-exposed berries and wine, limiting their usefulness in elaborating our understanding of smoke-taint. It should be noted that not all modified glycones would be compatible with the employed sample preparation. For instance, the alkaline SPE wash used in the Strata-X procedure was intended to remove polyphenolics, but it could just as easily remove and/or hydrolyze hydroxycinnamate-VP-glycoside, organic acid, and/or acetate ester conjugates. As such, the results reported herein do not preclude their existence, nor their potential relevance to smoke-taint. Suitable sample preparation strategies to screen for these compounds are currently being developed.

The use of fragmentation analysis to identify VP-glycosides is challenging, as demonstrated by the spectra obtained for structural isomers (*e.g.,* **h** *versus* **G9**/**G10**). However, the detailed glycone fragmentation outlined herein will be useful for samples that contain an abundance of VP-glycosides (Hayasaka et al., 2013), which are more likely to have detectable levels of the plausible modified glycones in the VP-glycoside database we developed.

3.5.2. Wine made from smoke-exposed berries

Wines made from the control and smoke-exposed sample groups were also evaluated. It was interesting to note that many of the identified VP-glycosides appeared to survive primary fermentation, while the putatively proposed non-VP glycosides (**G4–G6**; see Section 3.6) showed large changes in absolute response (Fig. 5).

3.6. Alternate glycosides

Notwithstanding the compounds identified herein, the paucity of observed VP-glycosides was surprising, in light of the reported concentrations of simple VP-glycosides (which exceeded our MDL by, in some instances, 1000-fold) in smoke-exposed berries (Dungey et al., 2011; Hayasaka et al., 2013). To determine if this was a limitation of the current method, the Pinot noir samples from vineyard 1 (see Supporting Information) were analyzed to determine their free and acid-labile VP content. Noestheden, et al. demonstrated quantitative recovery of free VPs liberated from VP-glycosides after acid-catalyzed hydrolysis (Noestheden et al., 2017). Therefore, a comparison of the total acid-labile VPs *versus* the SPE fraction containing VP-glycosides would provide an indication of the VP-glycosides present for each VP (Table 1). Using the guaiacol data as an example, it was observed that the total acid-labile pool in wine (103 ng/g) was not reflected in the SPE fraction (41.6 ng/g) known to contain the model VP-glycosides (Fig. 2 and Table S5). Similar results were observed for 4-ethyphenol, 4-methylguaiacol and *p*-cresol, with all results consistent between berries and wine. Coupled with the lack of VP-glycosides identified in the smoke-exposed samples, these results demonstrated that acid-labile VP conjugates beyond simple glycosides likely contribute to the overall presentation of smoke-taint in the Pinot noir samples analyzed.

Serendipitously, as part of the VP-glycoside screen (Section 3.5.1), several precursor ions were identified at elevated levels in the smoke-exposed berries that did not correlate to any of the VP-glycosides evaluated herein (Fig. 5). Three isobaric peaks of **G3** were elevated in smoke-exposed berries (**G2**, **G4**, **G5**). Fragmentation analysis of **G2** demonstrated a full complement of glycone fragments and the Y_0 and $Y_0 - CH_3^{\cdot}$ ions indicated a guaiacyl conjugate. Based on evidence for

Table 1
Free and acid-labile VP conjugates for Pinot noir berries exposed to smoke on-vine, and the wine made from those berries from vineyard 1. B – berries; W – wine; (−) – control group; (+) – smoke exposed group.

Compound	free VPs (ng/g)				acid-labile VP conjugates (ng/g)							
	B[1]		W[1]		B[1]		W[1]		B[2]		W[2]	
	−	+	−	+	−	+	−	+	−	+	−	+
4-Ethylguaiacol	–	–	–	–	5.70	10.3	–	–	–	–	–	–
4-Ethylphenol	–	–	–	–	23.6	40.1	29.1	42.1	11.9	26.7	15.2	23.8
4-Methylguaiacol	–	3.22	–	2.56	5.36	69.2	17.3	63.0	–	54.5	14.4	40.2
Eugenol	–	–	–	–	11.7	15.9	10.8	13.6	–	–	–	–
Guaiacol	–	7.55	–	2.44	–	25.1	48.3	103	–	71.5	10.7	41.6
o-Cresol	–	–	–	–	–	39.6	7.92	40.3	–	–	–	–
p-Cresol	2.14	12.2	–	4.54	36.1	182	59.5	134	21.8	142	51.5	104
Syringol	20.2	12.8	90.0	119	94.3	112	82.4	82.4	–	–	–	–

[1] Whole berry homogenate.
[2] SPE fraction demonstrated to contain model VP-glycosides during method development (Section 3.2, Strata-X SPE).

non-glucoside flavonoid glycosides (Castillo-Muñoz, Gómez-Alonso, García-Romero, & Hermosín-Gutiérrez, 2007) in *V. vinifera*, we synthesized guaiacyl-D-galactopyranoside, as a mixture of anomers, and guaiacyl-α-D-mannopyranoside. The galactoside and mannoside product ion spectra (Figs. S17–S19) were indistinguishable from those of the glucosides (Figs. S1/S3), but these compounds were not retention time matches for **G2**. Subsequent enzymatic treatment demonstrated that **G2** was a β-glucoside (Fig. S16). When combined, these results strongly suggested this was not a guaiacyl conjugate, despite the appearance of Y_0 and $Y_0 - CH_3^{\cdot}$ ions. With the thought that the VP portion of **G2** could be a structural isomer of guaiacol, 4-methoxyphenyl-β-D-glucopyranoside was synthesized, but again, while the fragmentation spectra were consistent (Fig. S22), it was not a retention time match for **G2**. While the 3-methoxyphenol isomer was also a plausible choice, it was not investigated since it would not support the generation of the $Y_0 - CH_3^{\cdot}$ ions through resonance as the 2- and 4-methoxy isomers do. The identity of **G2** is the subject of ongoing investigations.

In an analogous finding, while **G4** and **G5** were also isobars of **G3** that were sensitive to β-glucosidase, the absence of glycoside and $Y_0 - CH_3^{\cdot}$ fragments suggested that, even though they were elevated in smoke-exposed berries and wine, they are likely not simple glycosides (and possibly not guaiacyls). The demonstrated difference between control and smoke-exposed berries and wine marks the potential importance of **G2**, **G4** and **G5** to smoke taint and determining their identity is the subject of ongoing investigations.

G6 (Fig. 5) was identified as a phenyl-hexose-pentoside based on precursor *m/z*, but fragmentation analysis revealed a potential syringol aglycone (although lacking the expected radical anion fragments) and a low prevalence of glycone fragments, including none suggestive of a hexose-pentoside. Enzymatic analysis of **G6** demonstrated a susceptibility to α-L-arabinofuranosidase, which suggested this compound was an unknown arabinoside (Fig. S16).

The discovery of these putative non-VP glycosides highlighted a limitation of using the glycone to screen for VP-glycosides, as this will inherently misidentify non-VP glycosides. Therefore, screening for VP-glycosides in smoke-exposed berries and wine should include the glycone and aglycone. Although, care must be taken with this screening strategy as well, as accurate mass is required to confidently differentiate syringol and guaiacol, since they share a nominal mass isobar at *m/z* 123, for example.

4. Conclusions

The data presented herein constitute a complete method for the extraction, chromatographic separation and characterization of simple VP-glycosides in smoke-exposed *V. vinifera* berries and the wine made from those berries. The required method development included the synthesis and characterization of 16 model VP-glycosides, four of which are not reported previously. Our results demonstrated that the glycone and aglycone influence the fragmentation pattern of VP-glycosides. The use of full scan product ion spectra with high-resolution accurate mass spectrometry enabled the proposal of divergent fragmentation patterns for α- and β-anomers, as well as for rhamnosides/xylosides *versus* hexosides (glucose/galactose). The detailed fragmentation pattern of the synthesized VP-disaccharides will aid in the characterization of acyl-modified glycones that were not observed in the current study, but are hypothesized to exist, given their confirmed presence on flavonoid glycosides and anthocyanins in *V. vinifera*. Future use of Y_0 (and radical anion) fragments will better facilitate screening methods aimed at identifying the presumed modified VP-glycones, as well as non-glycoside VP conjugates. We showed, for the first time, empirical evidence for the existence of putative non-VP glycosides that were elevated in smoke-exposed berries and wine. Based on their disappearance during fermentation, it is plausible that such compounds could contribute more than simple VP-glycosides (which remained largely unchanged after primary fermentation) to the expression of smoke-taint in wines made using smoke-exposed berries.

Funding

MN acknowledges the MITACS Accelerate program, University Graduate Fellowship and the Walter C. Sumner Memorial Fellowship for funding. WFZ acknowledges the Natural Science and Engineering Research Council of Canada (Discovery Grant, 2016-03929, and Engage Grant, 509805-17) the British Columbia Wine Grape Council (research grant) for funding and the Canada Foundation for Innovation, Canada: John Evans Leaders Fund (project number 35246) and the British Columbia Knowledge Development Fund for supporting critical infrastructure. GAD thanks the Natural Science and Engineering Research Council for financial support and Compute Canada for access to computational resources. ERM is grateful for financial support provided by CONACYT-Mexico (Ph.D. Scholarship 472432).

Acknowledgements

MN and WZ would like to thank Supra Research & Development for GC-MS/MS access. We thank Sydney Morgan for her assistance with yeast preparation.

Conflict of interest

The authors declare no conflict of interest.

Appendix A. Supplementary data

Supplementary data associated with this article can be found, in the online version, at http://dx.doi.org/10.1016/j.foodchem.2018.03.097.

References

Barnaba, C., Dellacassa, E., Nicolini, G., Nardin, T., Malacarne, M., & Larcher, R. (2016). Free and glycosylated simple phenol profiling in Apulian Italian wines. *Food Chemistry, 206*, 260–266. http://dx.doi.org/10.1016/j.foodchem.2016.03.040.

Castillo-Muñoz, N., Gómez-Alonso, S., García-Romero, E., & Hermosín-Gutiérrez, I. (2007). Flavonol profiles of *Vitis vinifera* red grapes and their single-cultivar wines. *Journal of Agricultural and Food Chemistry, 55*(3), 992–1002. http://dx.doi.org/10.1021/jf062800k.

Domon, B., & Costello, C. E. (1988). A systematic nomenclature for carbohydrate fragmentations in FAB-MS/MS spectra of glycoconjugates. *Glycoconjugate Journal, 5*(4), 397–409. http://dx.doi.org/10.1007/BF01049915.

Dungey, K. A., Hayasaka, Y., & Wilkinson, K. L. (2011). Quantitative analysis of glycoconjugate precursors of guaiacol in smoke-affected grapes using liquid chromatography-tandem mass spectrometry based stable isotope dilution analysis. *Food Chemistry, 126*(2), 801–806. http://dx.doi.org/10.1016/j.foodchem.2010.11.094.

Fanzone, M., Zamora, F., Jofré, V., Assof, M., Gómez-Cordovés, C., & Peña-Neira, Á. (2012). Phenolic characterisation of red wines from different grape varieties cultivated in Mendoza province (Argentina). *Journal of the Science of Food and Agriculture, 92*(3), 704–718. http://dx.doi.org/10.1002/jsfa.4638.

Frisch, M. J., Trucks, G. W., Schlegel, H. B., Scuseria, G. E., Robb, M. A., Cheeseman, J. R., ... Hratchian, D. J. (2009). *Guassian 09*. Wallingford, CT: Gaussian, Inc.

Hayasaka, Y., Baldock, G. A., Pardon, K. H., Jeffery, D. W., & Herderich, M. J. (2010). Investigation into the formation of guaiacol conjugates in berries and leaves of grapevine *Vitis vinifera L. cv.* cabernet sauvignon using stable isotope tracers combined with HPLC-MS and MS/MS analysis. *Journal of Agricultural and Food Chemistry, 58*(4), 2076–2081. http://dx.doi.org/10.1021/jf903732p.

Hayasaka, Y., Baldock, G. A., Parker, M., Pardon, K. H., Black, C. A., Herderich, M. J., & Jeffery, D. W. (2010). Glycosylation of smoke-derived volatile phenols in grapes as a consequence of grapevine exposure to bushfire smoke. *Journal of Agricultural and Food Chemistry, 58*(20), 10989–10998. http://dx.doi.org/10.1021/jf103045t.

Hayasaka, Y., Dungey, K. A., Baldock, G. A., Kennison, K. R., & Wilkinson, K. L. (2010). Identification of a β-D-glucopyranoside precursor to guaiacol in grape juice following grapevine exposure to smoke. *Analytica Chimica Acta, 660*(1–2), 143–148. http://dx.doi.org/10.1016/j.aca.2009.10.039.

Hayasaka, Y., Parker, M., Baldock, G. A., Pardon, K. H., Black, C. A., Jeffery, D. W., & Herderich, M. J. (2013). Assessing the impact of smoke exposure in grapes: Development and validation of a HPLC-MS/MS method for the quantitative analysis of smoke-derived phenolic glycosides in grapes and wine. *Journal of Agricultural and Food Chemistry, 61*(1), 25–33. http://dx.doi.org/10.1021/jf305025j.

Hehre, W. J., Ditchfield, R., & Pople, J. A. (1972). Self—consistent molecular orbital methods. XII. Further extensions of Gaussian—Type basis sets for use in molecular orbital studies of organic molecules. *The Journal of Chemical Physics, 56*(5), 2257–2261. http://dx.doi.org/10.1063/1.1677527.

Hjelmeland, A. K., & Ebeler, S. E. (2015). Glycosidically bound volatile aroma compounds in grapes and wine: A review. *American Journal of Enology and Viticulture, 66*(1), 1–11. http://dx.doi.org/10.5344/ajev.2014.14104.

Hjelmeland, A. K., Zweigenbaum, J., & Ebeler, S. E. (2015). Profiling monoterpenol glycoconjugation in *Vitis vinifera L. cv.* Muscat of Alexandria using a novel putative compound database approach, high resolution mass spectrometry and collision induced dissociation fragmentation analysis. *Analytica Chimica Acta, 887*, 138–147. http://dx.doi.org/10.1016/j.aca.2015.06.026.

Hofmann, J., Hahm, H. S., Seeberger, P. H., & Pagel, K. (2015). Identification of carbohydrate anomers using ion mobility-mass spectrometry. *Nature, 526*(7572), 241–244. http://dx.doi.org/10.1038/nature15388.

Justesen, U. (2001). Collision-induced fragmentation of deprotonated methoxylated flavonoids, obtained by electrospray ionization mass spectrometry. *Journal of Mass Spectrometry, 36*(2), 169–178. http://dx.doi.org/10.1002/jms.118.

Kennison, K. R., Gibberd, M. R., Pollnitz, A. P., & Wilkinson, K. L. (2008). Smoke-derived taint in wine: The release of smoke-derived volatile phenols during fermentation of Merlot juice following grapevine exposure to smoke. *Journal of Agricultural and Food Chemistry, 56*(16), 7379–7383. http://dx.doi.org/10.1021/jf800927e.

Kennison, K. R., Wilkinson, K. L., Williams, H. G., Smith, J. H., & Gibberd, M. R. (2007). Smoke-derived taint in wine : Effect of postharvest smoke exposure of grapes on the chemical composition and sensory characteristics of wine. *Journal of Agricultural and Food Chemistry, 55*, 10897–10901. http://dx.doi.org/10.1021/jf072509k.

Kobata, A. (2013). Exo- and endoglycosidases revisited. *Proceedings of the Japan Academy. Series B, Physical and Biological Sciences, 89*(3), 97–117. http://dx.doi.org/10.2183/pjab.89.97.

Liu, Y., He, J., Zhang, R., Shi, J., & Abliz, Z. (2009). Study of the characteristic fragmentation behavior of hydroquinone glycosides by electrospray ionization tandem mass spectrometry with optimization of collision energy. *Journal of Mass Spectrometry, 44*(8), 1182–1187. http://dx.doi.org/10.1002/jms.1593.

Marana, S. R. (2006). Molecular basis of substrate specificity in family 1 glycoside hydrolases. *IUBMB Life, 58*(2), 63–73. http://dx.doi.org/10.1080/15216540600617156.

Mayr, C. M., Parker, M., Baldock, G. A., Black, C. A., Pardon, K. H., Williamson, P. O., ... Francis, I. L. (2014). Determination of the importance of in-mouth release of volatile phenol glycoconjugates to the flavor of smoke-tainted wines. *Journal of Agricultural and Food Chemistry, 62*(11), 2327–2336. http://dx.doi.org/10.1021/jf405327s.

Noestheden, M., Dennis, E. G., & Zandberg, W. F. (2018). Quantitating volatile phenols in Cabernet Franc berries and wine after on-vine exposure to smoke from a simulated forest fire. *Journal of Agricultural and Food Chemistry, 66*(3), 695–703. http://dx.doi.org/10.1021/acs.jafc.7b04946.

Noestheden, M., Thiessen, K., Dennis, E. G., Tiet, B., & Zandberg, W. F. (2017). Quantitating organoleptic volatile phenols in smoke-exposed *Vitis vinifera* berries. *Journal of Agricultural and Food Chemistry, 65*(38), 8418–8425. http://dx.doi.org/10.1021/acs.jafc.7b03225.

Parker, M., Black, C. A., Barker, A., Pearson, W., Hayasaka, Y., & Francis, I. L. (2017). The contribution of wine-derived monoterpene glycosides to retronasal odour during tasting. *Food Chemistry, 232*, 413–424. http://dx.doi.org/10.1016/j.foodchem.2017.03.163.

Parker, M., Osidacz, P., Baldock, G. A., Hayasaka, Y., Black, C. A., Pardon, K. H., ... Francis, I. L. (2012). Contribution of several volatile phenols and their glycoconjugates to smoke-related sensory properties of red wine. *Journal of Agricultural and Food Chemistry, 60*(10), 2629–2637. http://dx.doi.org/10.1021/jf2040548.

Ristic, R., Fudge, A. L., Pinchbeck, K. A., De Bei, R., Fuentes, S., Hayasaka, Y., ... Wilkinson, K. L. (2016). Impact of grapevine exposure to smoke on vine physiology and the composition and sensory properties of wine. *Theoretical and Experimental Plant Physiology, 28*(1), 67–83. http://dx.doi.org/10.1007/s40626-016-0054-x.

Ristic, R., Pinchbeck, K. A., Fudge, A. L., Hayasaka, Y., & Wilkinson, K. L. (2013). Effect of leaf removal and grapevine smoke exposure on colour, chemical composition and sensory properties of Chardonnay wines. *Australian Journal of Grape and Wine Research, 19*(2), 230–237. http://dx.doi.org/10.1111/ajgw.12017.

Ristic, R., van der Hulst, L., Capone, D. L., & Wilkinson, K. L. (2017). Impact of bottle aging on smoke-tainted wines from different grape cultivars. *Journal of Agricultural and Food Chemistry, 65*, 4146–4152. http://dx.doi.org/10.1021/acs.jafc.7b01233.

Sarry, J. E., & Günata, Z. (2004). Plant and microbial glycoside hydrolases: Volatile release from glycosidic aroma precursors. *Food Chemistry, 87*(4), 509–521. http://dx.doi.org/10.1016/j.foodchem.2004.01.003.

Schindler, B., Barnes, L., Renois, G., Gray, C., Chambert, S., Fort, S., ... Compagnon, I. (2017). Anomeric memory of the glycosidic bond upon fragmentation and its consequences for carbohydrate sequencing. *Nature Communications, 8*(973), 1–7. http://dx.doi.org/10.1038/s41467-017-01179-y.

Schymanski, E. L., Jeon, J., Gulde, R., Fenner, K., Ru, M., Singer, H. P., & Hollender, J. (2014). Identifying small molecules via high resolution mass spectrometry: Communicating confidence. *Environmental Science & Technology, 48*, 2097–2098. http://dx.doi.org/10.1021/es5002105 |.

Tikunov, Y. M., Molthoff, J., de Vos, R. C. H., Beekwilder, J., van Houwelingen, A., van der Hooft, J. J. J., ... Bovy, A. G. (2013). non-smoky glycosyltransferase1 prevents the release of smoky aroma from tomato fruit. *The Plant Cell, 25*(8), 3067–3078. http://dx.doi.org/10.1105/tpc.113.114231.

Wirth, J., Guo, W., Baumes, R., & Günata, Z. (2001). Volatile compounds released by enzymatic hydrolysis of glycoconjugates of leaves and grape berries from *Vitis vinifera* Muscat of Alexandria and Shiraz cultivars. *Journal of Agricultural and Food Chemistry, 49*(33), 2917–2923. http://dx.doi.org/10.1021/jf001398l.

Yang, W. Z., Qiao, X., Bo, T., Wang, Q., Guo, D. A., & Ye, M. (2014). Low energy induced homolytic fragmentation of flavonol 3-O-glycosides by negative electrospray ionization tandem mass spectrometry. *Rapid Communications in Mass Spectrometry, 28*(4), 385–395. http://dx.doi.org/10.1002/rcm.6794.

Zhao, Y., & Truhlar, D. G. (2008). The M06 suite of density functionals for main group thermochemistry, thermochemical kinetics, noncovalent interactions, excited states, and transition elements: Two new functionals and systematic testing of four M06-class functionals and 12 other function. *Theoretical Chemistry Accounts, 120*(1–3), 215–241. http://dx.doi.org/10.1007/s00214-007-0310-x.